Differential Uptake of Functionalized Polystyrene Nanoparticles by Human Macrophages and a Monocytic Cell Line

Oleg Lunov,[†] Tatiana Syrovets,[†] Cornelia Loos,[†] Johanna Beil,[†] Michael Delacher,[†] Kyrylo Tron,[‡] G. Ulrich Nienhaus,[§,⊥] Anna Musyanovych,[¶] Volker Mailänder,[¶] Katharina Landfester,[¶] and Thomas Simmet[†,*]

[†]Institute of Pharmacology of Natural Products & Clinical Pharmacology, and [‡]Institute of Biophysics, Ulm University, Ulm, Germany, [§]Institute of Applied Physics and Center for Functional Nanostructures, Karlsruhe Institute of Technology (KIT), Karlsruhe, Germany, [⊥]Department of Physics, University of Illinois at Urbana—Champaign, Illinois 61801, United States, and [¶]Max-Planck-Institute for Polymer Research, Mainz, Germany

ABSTRACT Tumor cell lines are often used as models for the study of nanoparticle—cell interactions. Here we demonstrate that carboxy (PS-COOH) and amino functionalized (PS-NH_2) polystyrene nanoparticles of ~100 nm in diameter are internalized by human macrophages, by undifferentiated and by PMA-differentiated monocytic THP-1 cells *via* diverse mechanisms. The uptake mechanisms also differed for all cell types and particles when analyzed either in buffer or in medium containing human serum. Macrophages internalized ~4 times more PS-COOH than THP-1 cells, when analyzed in serum-containing medium. By contrast, in either medium, THP-1 cells internalized PS-NH_2 more rapidly than macrophages. Using pharmacological and antisense *in vitro* knockdown approaches, we showed that, in the presence of serum, the specific interaction between the CD64 receptor and the particles determines the macrophage uptake of particles by phagocytosis, whereas particle internalization in THP-1 cells occurred *via* dynamin II-dependent endocytosis. PMA-differentiated THP-1 cells differed in their uptake mechanism from macrophages and undifferentiated THP-1 cells by internalizing the particles *via* macropinocytosis. In line with our *in vitro* data, more intravenously applied PS-COOH particles accumulated in the liver, where macrophages of the reticuloendothelial system reside. By contrast, PS-NH_2 particles were preferentially targeted to tumor xenografts grown on the chorioallantoic membrane of fertilized chicken eggs. Our data show that the amount of internalized nanoparticles, the uptake kinetics, and its mechanism may differ considerably between primary cells and a related tumor cell line, whether differentiated or not, and that particle uptake by these cells is critically dependent on particle opsonization by serum proteins.

KEYWORDS: phagocytes · polystyrene particles · surface chemistry · endocytosis · phagocytosis · clathrin · CD64

The rapid advancement of nanotechnology promoted the development of numerous nanomaterials, which often possess complex structures and surface functionalizations.[1−3] In biological systems, nanosized particles may play an ambivalent role. On one hand, they may elicit toxic side effects,[4] whereas, on the other hand, novel nanoscaled diagnostics and drug-delivery vehicles hold great promise for better medical treatment.[5] Especially the targeting of tumor and inflammatory cells for diagnostic and/or therapeutic reasons are of prime interest.

The bone marrow as origin of myeloid cells gives rise to monocytes, which upon emigration into tissues differentiate into macrophages.[6] This differentiation process concurs with the expression of various cellular receptors, which allow macrophages to efficiently sense and internalize particular material including nanoparticles.[6,7] Importantly, resident tissue macrophages are involved in all types of chronic inflammatory diseases including atherosclerosis, rheumatoid arthritis, and neuroinflammatory diseases, where they play a crucial role in the initiation and maintenance of the inflammatory process that ultimately leads to tissue destruction.[8,9] On this background, macrophages qualify as a prime target for therapeutic nanocarriers that might modulate chronic proinflammatory processes.[8] The specific development of therapeutic drug targeting to macrophages would be considerably facilitated if the mechanisms of interaction between the macrophage membrane and the nanoparticles as well as the subsequent uptake mechanisms were fully understood. In this context, modifications of the contact surface by distinct functionalization of nanosized materials provide an efficient tool to gain deeper insight into the mechanistic processes involved.

Unwanted interactions between diagnostic or therapeutic nanomaterials and macrophages of the reticuloendothelial system might also occur. This presents another motivation to strive for better insights into the characteristics and structural determinants governing the interaction between

* Address correspondence to thomas.simmet@uni-ulm.de.

Received for review August 9, 2010 and accepted February 9, 2011.

Published online February 23, 2011
10.1021/nn2000756

TABLE 1. Characterization of Carboxy and Amino Functionalized Polystyrene Nanoparticles Labeled with PMI as Fluorescent Dye[a]

particles	diameter nm	PDI	amount of groups (groups/nm^2)	zeta-potential (mV)	PMI contents (mg PMI/g polymer)
PS-COOH	116	0.01	0.130	-46 ± 7	0.40 ± 0.01
PS-NH_2	113	0.01	0.144	$+56 \pm 8$	0.51 ± 0.01

[a] Physical parameters of polystyrene nanoparticles were characterized by dynamic light scattering using a Zetasizer Nano and UV/vis absorption spectroscopy. PDI, polydispersity index; PMI, *N*-(2,6-diisopropylphenyl)-perylene-3,4-dicarbonacidimide.

distinct nanoparticles and macrophages. Indeed, macrophages are multifunctional phagocytic cells, which are fully equipped to sense and internalize endogenous and exogenous material, such as viruses, microorganisms, cells, cell debris, and foreign particulate matter including a variety of engineered nanoparticles.[6,8,10] Recognition and uptake of designed nanoparticles by macrophages is useful, of course, when, for example, nanoparticular iron oxide such as ferucarbotran is employed for magnetic resonance imaging of hepatic lesions.[11] Yet, such uptake would be undesirable, if TNF-covered nanosized gold particles intended to target solid tumor cells[5] accumulated in reticuloendothelial macrophages.

Studies on the interaction of nanoparticles with monocytic cell lines such as THP-1 or U937 may be clearly motivated as long as they serve the development of drug-loaded nanoparticles for the treatment of leukemia. However, due to their convenient availability, monocytic cell lines of varying degrees of differentiation have often been used as surrogates of human macrophages *in vitro*.[12−14] In fact, differentiation can be induced in monocytic cell lines with phorbol-12-myristate-13-acetate (PMA) or 1,25-dihydroxyvitamin D_3. Such differentiated cell lines exhibit enhanced expression of macrophage surface markers and can more efficiently take up bacteria by phagocytosis compared to undifferentiated cells.[15,16] Nevertheless, the phenotype of the differentiated cells differs from that of macrophages, reflecting differences in gene expression between the monocytic cell lines and macrophages.[15,17] Therefore, it remains doubtful to which extent monocytic cells represent a useful model for macrophages as far as mechanistic aspects of nanoparticle−cell interaction or cellular uptake mechanisms are concerned. We addressed this question by studying the uptake of defined nanoparticles by human macrophages and, for comparison, to undifferentiated and differentiated THP-1 cells.

Polystyrene nanoparticles can be easily synthesized in a wide range of sizes, which facilitates their application as biosensors,[18] in photonics,[19] and in self-assembling nanostructures.[20] Specific surface modifications, high drug loading capacity, and colloidal stability in biological media also contribute to their application as experimental drug carrier systems.[21] Due to their size homogeneity and the ease of surface modifications, we have used polystyrene nanoparticles as model particles for our experiments. Surface functionalization of nanoparticles is crucial for the durability, suspensibility in biological media, biocompatibility, and biodistribution.[22,23] Compared to amino and thiol residues, functionalization with carboxyl groups renders nanoparticles more suitable for further conjugation with oligonucleotides, antibodies, or other proteins.[24] On the other hand, functionalization of nanoparticles with primary amines offers a high gene delivery efficiency, since it exhibits a unique "proton-sponge"[25] or "endosome buffering" effect",[26] thus destabilizing lysosomal membranes and promoting escape from endosomal to cytoplasmic localization. Besides, functionalization of nanoparticles with amino groups might reduce their uptake into macrophages.[27] In general, it remains a particular challenge to produce nanoparticles for biomedical applications, especially for applications *in vivo*, if unwanted particle uptake by macrophages is a concern.

Considering the importance of particle functionalization for their controlled and targeted biomedical applications, the aim of this study was to gain insight into the uptake mechanism of carboxy and amino functionalized polystyrene nanoparticles by human macrophages in comparison to the uptake by the monocytic cell line THP-1 as well as differentiated THP-1 cells.

RESULTS AND DISCUSSION

Preparation of Polystyrene Nanoparticles and their Physicochemical Characterization. In this study, two types of fluorescent polystyrene nanoparticles were used that were synthesized by the miniemulsion process.[28,29] The physicochemical properties of the nanoparticles were characterized by dynamic light scattering, UV/vis absorption spectroscopy and are summarized in Table 1. Both particles had the same mean hydrodynamic diameter of about 110 nm. The high negative or positive zeta potential reflected the functionalization of the particles either with carboxy or amino groups, respectively. Both particles had approximately the same surface density of charged groups and contained basically the same amount of the fluorescent dye PMI, which was incorporated into the particles during their synthesis (Table 1). Similar physicochemical characteristics of the particles and the low polydispersity index

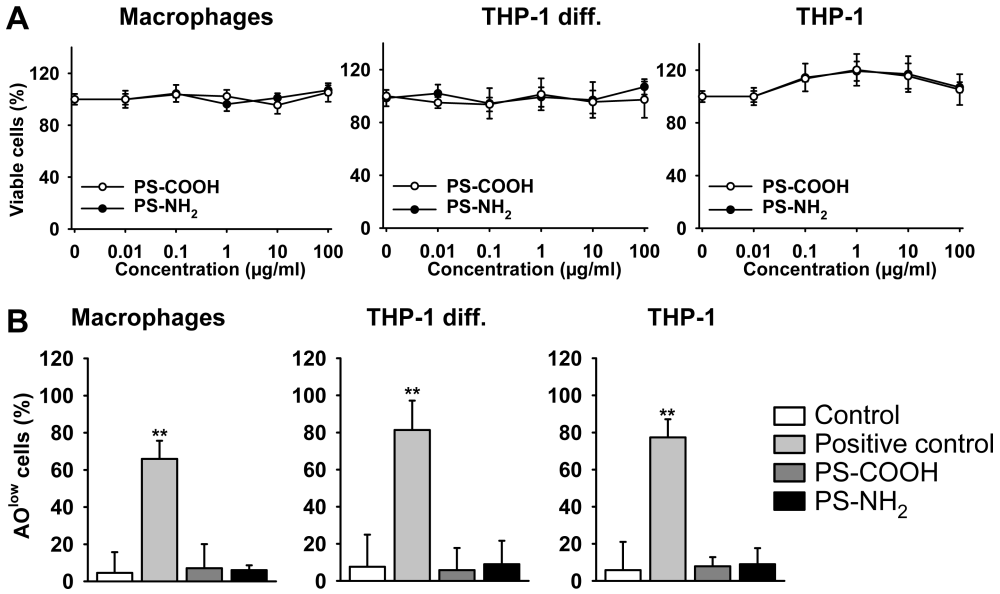

Figure 1. Polystyrene nanoparticles are nontoxic for human macrophages, undifferentiated, and PMA-differentiated THP-1 cells. (A) The cells were cultured in RPMI 1640 supplemented with 10% human AB serum for 48 h in the presence or absence of PS-COOH or PS-NH_2 polystyrene nanoparticles. Cell viability was assessed by the XTT assay. The data were normalized to control values (no particle exposure) and expressed as mean ± SEM, n = 3 each. (B) Polystyrene nanoparticles do not affect lysosomal integrity. The cells were treated for 48 h with polystyrene particles (100 μg/mL) as in panel A, stained with acridine orange (AO), and analyzed by flow cytometry to detect the population of AO^{low} cells exhibiting leaking lysosomes. Positive control, 1 μM camptothecin for 4 h. All data are expressed as mean ± SEM of at least 3 independent experiments.

allowed us to analyze the role of surface charge on the uptake kinetics and the uptake mechanisms of the particles by macrophages and THP-1 cells.

Kinetics of Nanoparticle Internalization. Upon application, the majority of nanoparticles are finally sensed and internalized by macrophages.[8,30] Surface functionalization greatly influences particle recognition and uptake by macrophages. Hence, it is important to analyze particle properties, which might facilitate or impede their uptake by macrophages. Because primary tissue macrophages cannot be readily expanded *ex vivo*, monocytic cell lines of varying degrees of differentiation have frequently been used to model macrophage functions.[14]

Owing to their advanced differentiation state, monocytic THP-1 cells are often used as surrogates of *in vitro* macrophages[12,31] to study the uptake of nanoparticles.[32−34] Originally isolated from a patient suffering from acute monocytic leukemia, THP-1 cells express a number of hematopoietic differentiation markers and can be classified as immature macrophages.[12] Nevertheless, such a monocytic cell line might differ from primary cells in terms of surface receptor expression and uptake mechanisms. Indeed, THP-1 cells exhibit a reduced phagocytic capacity compared to macrophages.[15,16]

To ensure that the particles do not exert any toxicity on the cells during the experiments, we first analyzed the effects of the nanoparticles on cell viability. Human macrophages, undifferentiated THP-1, and PMA-differentiated THP-1 cells cultured in medium for 48 h in the presence or absence of PS-COOH or PS-NH_2 nanoparticles did not show any significant changes in cell viability nor lysosomal leakage (Figure1A,B). This finding is at variance with a previous study reporting that smaller cationic polystyrene nanoparticles might induce lysosomal leakage and ROS production in a murine macrophage cell line. Interestingly, the toxicity of these particles was dependent on the cell line used and the uptake mechanism,[13,14] although surfactant residues might also have played a critical role.

The majority of uptake studies *in vitro* have been performed in buffers devoid of protein. In physiological fluids, however, a protein corona could be formed on a particle surface and affect its interaction with cells.[23,35,36] To analyze the effect of particle opsonization by human serum proteins, we performed uptake studies either in Ca^{2+}/Mg^{2+}-containing HBSS or in cell culture medium supplemented with 10% human AB serum.

The particles used in this study contained fluorescent dye trapped within the particles during synthesis. This enabled analysis of particle uptake by the cells using flow cytometry because the cell fluorescence correlates with the amount of internalized nanoparticles. A rigorous washing protocol controlled by 3D confocal microscopy actually ensured that all noninternalized particles had been removed from the cell surface prior to flow cytometric analysis (Figure S1, Supporting Information). Both types of nanoparticles were taken up by the cells, although to a different extent. After 3−6 h of incubation in buffer, THP-1 cells took up about 38% more PS-COOH than macrophages (Figure 2A). Both cell types internalized about the same amounts of PS-NH_2, although THP-1 cells incorporated

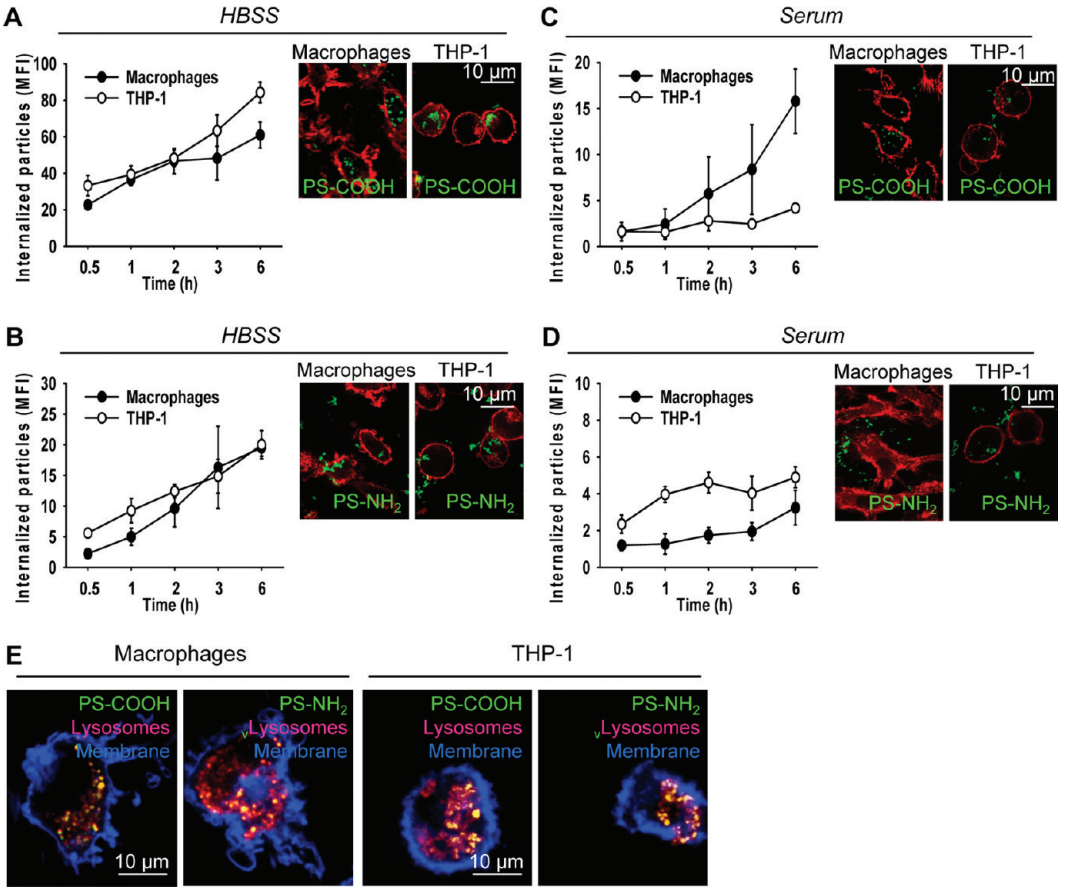

Figure 2. Uptake kinetics of carboxy and amino functionalized polystyrene nanoparticles by human macrophages and THP-1 cells. The cells were incubated with PS-COOH (A) or PS-NH_2 (B) nanoparticles (each at 100 μg/mL) in HBSS for the indicated time and washed, and the particle uptake was analyzed by flow cytometry. Increased cell fluorescence due to accumulation of fluorescent nanoparticles is presented as mean fluorescence index (MFI). Results are given as mean $\pm$ SEM, n = 3. Cells cultured in RPMI 1640 with 10% human AB serum were treated with PS-COOH (C) or PS-NH_2 (D) nanoparticles (each at 100 μg/mL) and analyzed as in panel A. Photomicrographs show cells incubated with the indicated nanoparticles (100 μg/mL) for 2 h and analyzed using confocal microscopy (cell membranes, CellMask (red); nanoparticles, PMI (green); original magnification 640×). (E) Accumulation of polystyrene nanoparticles in lysosomes. Human macrophages and THP-1 cells were incubated with PS-COOH or PS-NH_2 (each at 100 μg/mL) for 2 h and analyzed by confocal microscopy (cell membranes, CellMask (blue); lysosomes, LysoTracker Red DND-99 (red); nanoparticles, PMI (green); colocalization (yellow); original magnification 800×).

the particles more rapidly than macrophages (Figure 2B). Both cell types took up significantly less PS-NH_2 than PS-COOH nanoparticles when analyzed in HBSS (Figure 2A,B).

In serum-containing medium, macrophages and THP-1 cells internalized much less nanoparticles than in buffer (Figure 2A−D). Differently to buffer, in the presence of serum, macrophages took up about four times more PS-COOH nanoparticles than THP-1 cells (Figure 2C). THP-1 cells, in turn, internalized PS-NH_2 in larger amounts and more quickly than macrophages (Figure 2D). We further validated those flow cytometric data by confocal microscopy, demonstrating that the particles were indeed internalized by the cells and localized intracellularly in particular in the lysosomal compartment (Figure 2A−E and Supporting Information, Figure S1). The considerable differences in nanoparticle uptake in the absence or presence of serum, the latter leading to opsonization, suggested that differential endocytic mechanisms might be involved.

Analysis of the Endocytic Mechanisms. Macrophages are professional phagocytes. Unlike other cells, they are capable of efficient uptake of particles by phagocytosis. Macrophages express a number of receptors, such as FcR and complement receptors, which may facilitate such processes. The optimal particle size for phagocytosis is relatively large, 250 nm to 3 μm for polystyrene particles.[7] In contrast to phagocytosis, endocytosis occurs in virtually all cells and is indispensible for intercellular communication and nutrient uptake.[7] Endocytosis can occur, for example, *via* engagement of clathrin or caveolin pits. Clathrin- or caveolin-independent but dynamin-dependent endocytosis has also been described.[7] Caveolin is barely expressed by human macrophages, but can be induced, for example, by treatment with agonists of liver X nuclear receptors.[37] It is generally accepted that the size of endocytotic pits is restricted to about 120 nm. Therefore, particles of larger diameter cannot be taken up by endocytosis. However, studies on cellular uptake of

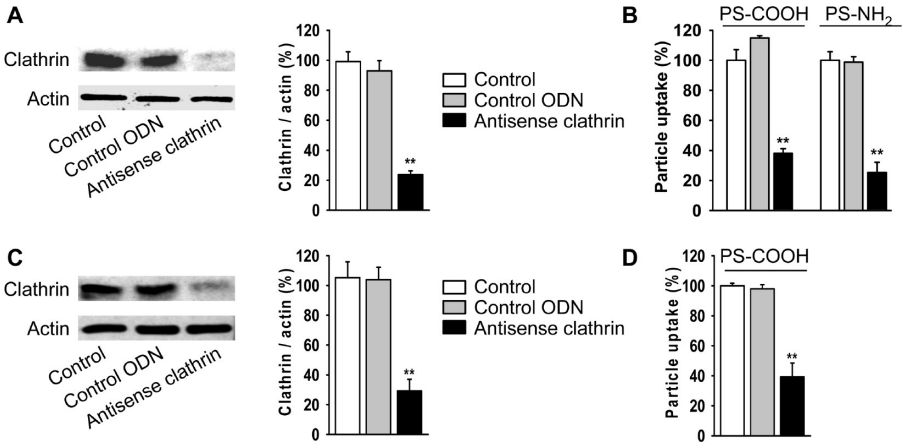

Figure 3. The role of clathrin-dependent endocytosis in the uptake of particles by THP-1 cells and macrophages cultured in HBSS. Antisense ODN downregulate the expression of clathrin in THP-1 cells (A) and macrophages (C). After treatment with ODN against clathrin or the control sequence for 48 h, the clathrin expression was determined by immunoblotting; actin = loading control. Graphs show the densitometric analysis of the immunoblots. Treatment with clathrin antisense ODN inhibits the nanoparticle uptake in THP-1 cells (B) and macrophages (D) cultured in HBSS (analyzed by flow cytometry as in Figure 2A,B); (**) $p < 0.01$ *versus* controls, mean ± SEM, $n = 3$.

bacteria and viruses demonstrated that this limitation may not be strictly obeyed, and that a cell might, indeed, also take up larger particles by endocytosis due to engagement of various receptors.[38]

To obtain evidence of the mechanistic nature of nanoparticle uptake, macrophages and THP-1 cells were pretreated with different uptake inhibitors prior to particle incubation. Polyinosinic acid was used to inhibit scavenger receptors type A,[32] rottlerin as an inhibitor of macropinocytosis,[39] pinocytosis was inhibited with colchicine,[40] cytochalasin B was used as an inhibitor of phagocytosis,[40] clathrin-mediated endocytosis was inhibited by monodansyl cadaverine,[41] caveolae-mediated endocytosis by nystatin,[42] and dynamin-dependent endocytosis was inhibited by dynasore.[43] In preliminary experiments we ensured that the inhibitors did not affect cell viability at the concentrations used (Supporting Information, Figure S2).

In buffer, PS-COOH particle uptake by macrophages was significantly inhibited by monodansyl cadaverine and dynasore suggesting that macrophages may internalize the negatively charged particles mainly *via* clathrin- and dynamin-dependent endocytosis (Supporting Information, Figure S3A), whereas the PS-NH_2 were apparently taken up *via* macropinocytosis (Supporting Information, Figure S3B). In contrast to macrophages, THP-1 cells did not differentiate between the particle charge under buffer conditions and took up both, PS-COOH and PS-NH_2, by macropinocytosis (inhibition of uptake with rottlerin) and clathrin- and dynamin-dependent endocytosis (inhibition of uptake with monodansyl cadaverine and dynasore) (Supporting Information, Figure S3A,B). This uptake mechanism differs from that described for rat alveolar epithelial cells, which internalized more positively charged PS particles of 100 nm than negatively charged ones; these processes were not inhibited by inhibitors of endocytosis.[44] Human mesenchymal cells isolated from bone marrow aspirates of human donors took up positively charged PS particles of 100 nm by clathrin-dependent endocytosis,[43] resembling THP-1 cells rather than macrophages.

Due to the limited specificity of pharmacological inhibitors, these results were further validated and confirmed with a different set of structurally and functionally different inhibitors of pinocytosis, macropinocytosis, and phagocytosis, namely nocodazole,[45] dimethylamiloride,[46] and latrunculin A[47] (Supporting Information, Figure S4A–D). The specificity of the inhibitors used to inhibit clathrin- and dynamin-dependent endocytosis was confirmed by analyzing the uptake of fluorescently labeled transferrin by macrophages. As expected, monodansyl cadaverine and dynasore[48] inhibited transferrin uptake by macrophages, which was used as a readout of clathrin- and dynamin-dependent endocytosis, whereas the inhibitors of pinocytosis, macropinocytosis, phagocytosis, and caveolin-mediated endocytosis remained ineffective (Supporting Information, Figure S4E).

To confirm those data, we knocked down the expression of clathrin by treatment of THP-1 cells and macrophages with phosphothioate-modified oligodeoxynucleotides (ODN) designed to target clathrin mRNA. In control experiments, clathrin antisense ODN had been shown to specifically inhibit clathrin-dependent endocytosis of transferrin without affecting clathrin-independent phagocytosis of bacteria (Supporting Information, Figure S5). Clathrin antisense ODN inhibited the clathrin expression by 76.2 ± 2.6% in THP-1 cells (Figure 3A) and by 70.8 ± 7.8% in macrophages (Figure 3C). Besides, clathrin antisense ODN significantly reduced uptake of PS-COOH by 62.2 ± 3.2% and that of PS-NH_2 by 75.9 ± 6.7% by THP-1 (Figure 3B), and uptake of PS-COOH by macrophages

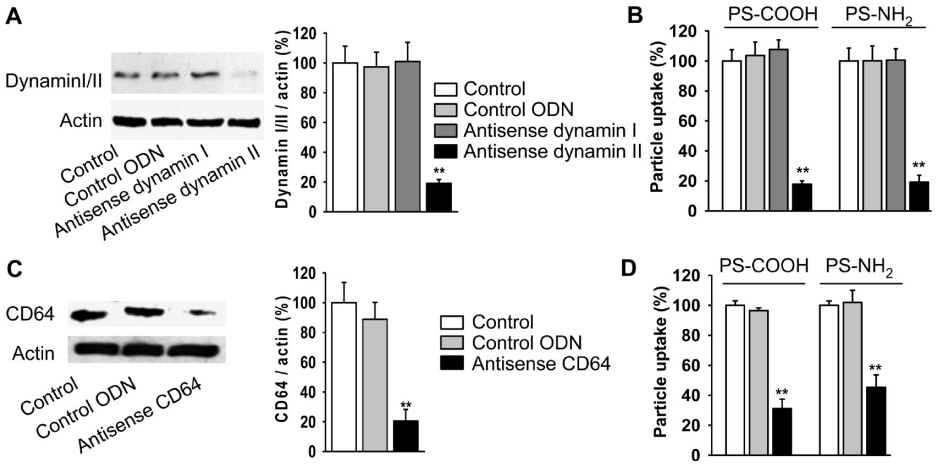

Figure 4. THP-1 cells internalize particles by dynamin II-dependent endocytosis; human macrophages internalize particles by CD64-dependent phagocytosis. (A) Antisense ODN downregulate the expression of dynamin II in THP-1 cells. After treatment with ODN against dynamin I, dynamin II, or control sequence for 24 h, dynamin expression was determined by immunoblotting; actin = loading control. Antisense to dynamin I, which is not expressed by THP-1 cells, was used to ensure specificity of the downregulation. Graph shows the densitometric analysis of the immunoblots. (B) Treatment with antisense ODN against dynamin II inhibits uptake of nanoparticles by THP-1 cells (analyzed in serum-containing medium by flow cytometry as in Figure 2C,D). (C) Antisense ODN downregulate the expression of CD64 in macrophages. After treatment with ODN against CD64 and control sequence for 48 h, CD64 expression was determined by immunoblotting; actin = loading control. Graph shows the densitometric analysis of the immunoblots. (D) Treatment with antisense ODN against CD64 inhibits uptake of nanoparticles by macrophages (analyzed in serum-containing medium by flow cytometry as in Figure 2C,D); (**) $p < 0.01$ *versus* controls, mean ± SEM, $n = 3$.

by 61.3 ± 9.2% (Figure 3D), clearly confirming the preliminary data obtained with the pharmacological uptake inhibitors.

By contrast, in the presence of human AB serum, macrophages apparently internalized both nanoparticles mainly by phagocytosis (uptake inhibition by cytochalasin B), whereas THP-1 cells apparently took up both nanoparticles by dynamin-dependent endocytosis (uptake inhibition by dynasore) (Supporting Information, Figure S3C,D). In addition, a small amount of PS-NH_2 nanoparticles might have been internalized by macrophages *via* caveolin- and dynamin-dependent endocytosis (Supporting Information, Figure S3D). The size of the nanoparticles might also affect the uptake mechanism. Thus, 50 nm polystyrene particles preincubated with plasma proteins were internalized by Kupffer cells (liver macrophages) *via* scavenger receptors, with the plasma protein fetuin mediating this uptake.[49]

Dynamin is a guanosine triphosphatase that has been implicated in clipping clathrin-coated invaginations from the plasma membrane. Three distinct dynamin genes have been identified in mammals. Their products, dynamin I, II, and III have similar primary structures and functions, but exhibit differences in tissue distribution. Only dynamin II was found in all tissues analyzed.[50,51] To validate the involvement of dynamin in the particle internalization by THP-1 cells, we knocked down dynamin expression by treatment of the cells with ODN designed to target dynamin I and II mRNA. Antisense ODN against dynamin I, which is expressed exclusively in neurons,[50,51] and scrambled ODN were used as controls of specific dynamin II targeting.

Antisense ODN against dynamin II inhibited expression of dynamin II in THP-1 cells by 81.0 ± 2.6% (Figure 4A) and, concomitantly, reduced cellular uptake of PS-COOH by 82.2 ± 2.2% and PS-NH_2 by 80.9 ± 4.6%, confirming that particle uptake by THP-1 cells occurs in a dynamin II-dependent manner (Figure 4B).

Macrophages, as professional phagocytes, can efficiently recognize and internalize particles *via* phagocytosis. Labeling of the particles by plasma proteins, mainly antibodies and complement components, initiates particle recognition by specific receptors essential for phagocytosis.[7] CD64, a high affinity Fc receptor, belongs to a group of immunoglobulin receptors widely expressed on immune cells and involved in phagocytosis. Activation of Fc receptors might activate or inhibit immune responses, and loss in this balanced signaling results in tissue damage and autoimmune diseases.[52]

Macrophages pretreated with antisense ODN against CD64 exhibited a decreased expression of this receptor by 85.5 ± 7.8% (Figure 4C) and an impaired internalization of the nanoparticles by 68.2 ± 6.4% and 54.7 ± 8.3% for PS-COOH and PS-NH_2, respectively (Figure 4D), indicating that in the presence of human plasma proteins, macrophages phagocyte polystyrene nanoparticles primarily *via* the immunoglobulin receptor CD64.

PMA-Differentiated THP-1 Cells Take up Nanoparticles by a Different Mechanism. PMA, which activates protein kinase C, is commonly used to induce macrophage-like differentiation in monocytic cell lines.[15,16] PMA treatment results in acquisition of an adherent growth phenotype, loss of proliferation, phagocytosis of latex

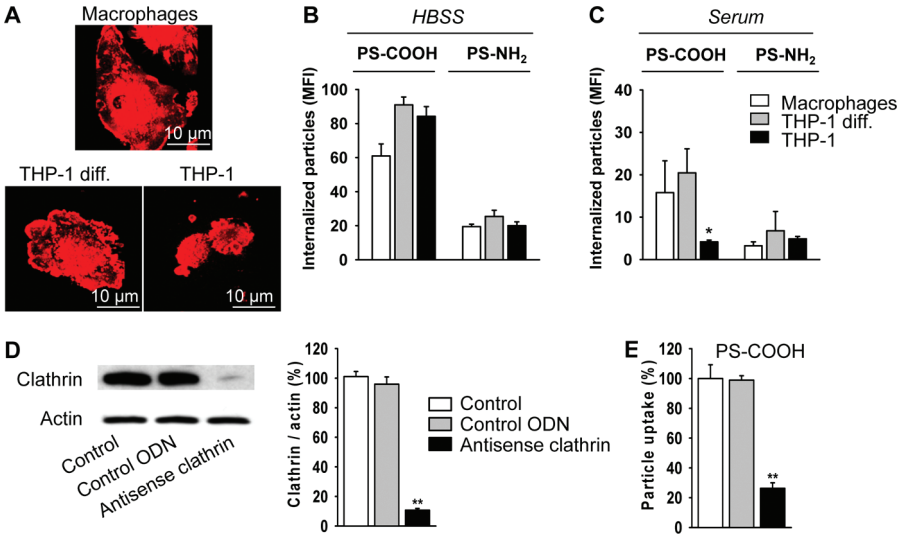

Figure 5. Comparison of the uptake of carboxy and amino functionalized polystyrene nanoparticles by human macrophages, THP-1, and PMA-differentiated THP-1 cells. (A) Cell morphology as analyzed by confocal microscopy. Membranes of macrophages, PMA-differentiated THP-1 cells, and THP-1 cells were labeled with CellMask, and the cells were analyzed using confocal microscopy. Original magnification 900×. (B) The cells were incubated either with PS-COOH or PS-NH_2 (both at 100 μg/mL) in HBSS for 6 h, washed, and analyzed by flow cytometry. (C) The cells were incubated either with PS-COOH or PS-NH_2 (both at 100 μg/mL) in RPMI 1640 with 10% human AB serum and analyzed by flow cytometry as in panel B. (D) Antisense ODN downregulate the expression of clathrin in PMA-differentiated THP-1 cells. After treatment with ODN against clathrin or the control sequence for 48 h, clathrin expression was determined by immunoblotting; actin = loading control. The graph shows the densitometric analysis of the immunoblots. (E) Treatment with antisense ODN against clathrin inhibits uptake of PS-COOH particles by PMA-differentiated THP-1 cells in HBSS as analyzed by flow cytometry; (**) $p < 0.01$ *versus* controls, mean ± SEM, $n = 3$.

beads, and expression of surface macrophage markers, reflecting a more differentiated phenotype compared to nondifferentiated cells.[15,16] When compared to other differentiation protocols, PMA treatment promotes a more differentiated phenotype of THP-1 cells, which makes such cells more suitable for use as a macrophage model.[15,16] Differentiation of THP-1 cells with PMA increases the phagocytic activity of the cell,[15] although it still does not reach the level of human macrophages.[16]

On this background, we further analyzed whether differentiated THP-1 cells might better mimic macrophages with respect to polystyrene nanoparticle internalization. Differentiation with PMA induced an adherent cell phenotype and inhibited cell proliferation. Hence, the morphology of the three cell types analyzed in this study, that is, macrophages, undifferentiated THP-1 cells, and differentiated THP-1 cells, still remained different. THP-1 cells grow as small round cells in suspension, whereas macrophages are large and adherent. PMA-differentiated THP-1 cells also acquired an adherent phenotype, but significantly differed in size from macrophages (Figure 5A, Supporting Information, Figure S1).

The amount of PS-COOH internalized by macrophages and differentiated THP-1 cells in the presence of serum was similar, whereas, consistent with the previous observation (see Figure 2C), undifferentiated THP-1 cells internalized significantly less PS-COOH nanoparticles (Figure 5C). The uptake of PS-NH_2 nanoparticles was similar among primary macrophages, PMA-differentiated THP-1, and undifferentiated THP-1 cells (Figure 5C).

The effects of uptake inhibitors suggested that differentiated THP-1 cells internalized PS-COOH in HBSS *via* scavenger receptor-, clathrin-, and dynamin-dependent endocytosis (Supporting Information, Figure S6A). Although macrophages took up PS-COOH also in a clathrin- and dynamin-dependent manner, they did not seem to use the scavenger receptor. Under those buffer conditions, macropinocytosis appeared to play a predominant role in the uptake of PS-NH_2 nanoparticles by both macrophages and differentiated THP-1 cells (Supporting Information, Figures S3B and S6A,C). When the experiments were performed in serum-containing medium, differentiated THP-1 cells apparently took up both nanoparticles *via* macropinocytosis, whereas macrophages incorporated them mainly *via* CD64-dependent phagocytosis (Figure 4D, Supporting Information, Figure S3C,D, S4C,D and S6B,D). PS-NH_2 particle uptake by differentiated THP-1 cells proceeded obviously exclusively through macropinocytosis, whereas undifferentiated THP-1 cells also employed clathrin- and dynamin-dependent endocytosis (Supporting Information, Figure S3B and S6A,C). The differences between undifferentiated and differentiated THP-1 were more pronounced if the uptake was analyzed in serum-containing medium. THP-1 cells apparently took up the particles *via* dynamin-dependent endocytosis, whereas PMA-differentiated THP-1 cells

TABLE 2. Mechanisms Involved in the Uptake of PS-COOH and PS-NH_2 Particles by Macrophages and Differentiated or Undifferentiated Monocytic THP-1 Cells[a]

		medium			
		HBSS		RPMI 1640/10% serum	
particles	cell type				
PS-COOH	macrophages	endocytosis	clathrin-MDC_+, ODN_+ dynamin−Dyn_+	phagocytosis	Cyt B_+, Lat A_+, CD64−ODN_+
	differentiated THP-1	endocytosis	clathrin−MDC_+, dynamin−Dyn_+	macropinocytosis	Rot_+, DMA_+
		endocytosis (SR)	PIA_+		
	THP-1	endocytosis	clathrin−MDC_+, ODN_+, dynamin−Dyn_+	endocytosis	dynamin−Dyn_+, ODN_+
		macropinocytosis	Rot_+, DMA_+		
PS-NH_2	macrophages	macropinocytosis	Rot_+, DMA_+	phagocytosis	Cyt B_+, Lat A_+, CD64−ODN_+ Dyn_+, Nys_+
	differentiated THP-1	macropinocytosis	Rot_+, DMA_+	macropinocytosis	Rot_+, DMA_+
	THP-1	endocytosis	clathrin− MDC_+, ODN_+ dynamin−Dyn_+	endocytosis	dynamin−Dyn_+, ODN_+
		macropinocytosis	Rot_+, DMA_+		

[a] Cyt B, cytochalasin B; DMA, dimethylamiloride; Dyn, dynasore; Lat A, latrunculin A; MDC, monodansyl cadaverine; Nys, nystatin; ODN, antisense desoxynucleotides; PIA, polyinosinic acid; Rot, rottlerin; SR, scavenger receptor-A; +, sensitive.

via macropinocytosis (Supporting Information, Figure S3C,D and S6B,D).

To validate the involvement of clathrin in the PS-COOH particle internalization by differentiated THP-1 cells in buffer, we knocked down the clathrin expression with ODN targeting clathrin mRNA. Clathrin antisense ODN inhibited the expression of clathrin by 89.7 ± 1.2% (Figure 5D) and reduced the cellular uptake of PS-COOH by 77.3 ± 3.7% (Figure 5E).

Thus, although differentiated THP-1 cells internalize particles to the same extent as macrophages, they use distinctly different mechanisms for this function. To provide a synopsis, the major mechanisms taking part in the uptake of functionalized polystyrene nanoparticles by macrophages and differentiated as well as undifferentiated monocytic THP-1 cells are summarized in Table 2.

Particle Opsonization by Serum Proteins. The uptake mechanisms used by the cells was different for buffer and serum-containing medium. This observation indicates that particle interaction with plasma proteins played a crucial role in the uptake mechanism of the nanoparticles by either cell type. Proteins and other biomolecules are known to adsorb to the surfaces of nanoparticles thereby generating the so-called "protein corona".[35,53] Therefore, we analyzed the proteins that associated with the nanoparticles in HBSS *versus* medium containing human serum that might be responsible for the differences in the uptake mechanisms.

Whereas particles incubated in HBSS did not carry any proteins, multiple protein bands could be eluted from those particles that had been incubated in serum-containing medium (Figure 6A). Interestingly, the PS-COOH particles bound more and different proteins compared to PS-NH_2 (Figure 6A). Western blot analysis revealed that both particles bind plasma antibodies (Figure 6B). These data are in agreement with a previous report demonstrating that negatively charged polystyrene nanoparticles absorb about twice as much protein as positively charged particles of about 100 nm in diameter.[53] In addition, 2D protein gel electrophoresis showed that IgG immunoglobulins along with albumin constitute the major protein group found on the surface of these particles.[53]

In agreement with the uptake inhibition studies, macrophages express more CD64, the high affinity Fc receptor for IgG compared to nondifferentiated THP-1 cells. Macrophages express more CD64 protein in whole cell lysates as shown by Western blot analysis, and they also express more CD64 on the cell surface as analyzed by flow cytometry of non-permeabilized cells (Figure 6C,D). Differentiated THP-1 cells express similar amounts of CD64 as macrophages, but more scavenger receptor A (Figure 6C,D). The differences in cell surface expression of the receptors involved in nanoparticle internalization might, therefore, account for the differences in the uptake mechanisms that we observed between human macrophages, and differentiated and undifferentiated THP-1 cells.

Our data indicate that the uptake of PS-COOH and PS-NH_2 by macrophages in buffer does not involve phagocytosis, probably due to the absence of opsonizing plasma proteins and the smaller effective size of the nanoparticles. In the presence of human serum,

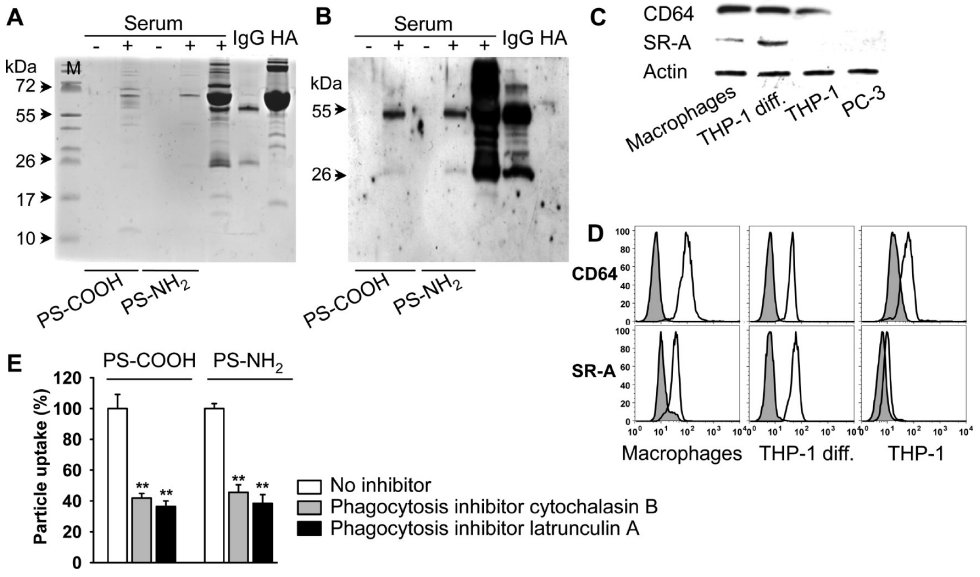

Figure 6. Opsonization of carboxy and amino functionalized polystyrene nanoparticles in the presence of human serum. PS-COOH or PS-NH_2 nanoparticles (100 μg/mL) were incubated either in HBSS (−) or in RPMI 1640 with 10% human AB serum (serum) for 1 h at 37 °C. The particles were collected by centrifugation and washed with PBS. Proteins associated with the particles were eluted and denatured in sample loading buffer and separated by gel electrophoresis. As controls, 0.5 μL of human AB serum, 2.5 μg of human IgG, and 50 μg of albumin (HA) were used. (A) The gel was stained with Coomassie blue or (B) blotted onto a PVDF membrane and stained with antihuman IgG-HRP. Arrows show the positions of heavy and light chains of IgG; M = molecular weight marker. Representative gels out of three. (C) Fcγ receptor CD64 and scavenger receptor A were analyzed in whole cell lysates of macrophages, PMA-differentiated THP-1, THP-1, and PC-3 cells by immunoblotting; actin = loading control. (D) Expression of Fcγ receptor CD64 and scavenger receptor A (empty peaks) as analyzed by flow cytomentry; gray peaks = isotype controls. A representative experiment out of three is shown. (E) Human macrophages take up nanoparticles opsonized with human IgG by phagocytosis. PS-COOH or PS-NH_2 were preincubated with 10 mg/mL human IgG for 2 h. Macrophages were pretreated with different phagocytosis inhibitors, and exposed to IgG-preincubated PS-COOH or PS-NH_2 nanoparticles (each at 100 μg/mL) in HBSS for 6 h, washed, and analyzed by flow cytometry. Phagocytosis inhibitors: 10 μg/mL cytochalasin B for 2 h and 0.5 μM latrunculin A for 30 min. Results are given as mean ± SEM, n = 3.

opsonization occurs and charged nanoparticles adsorb different proteins onto their surface. To further strengthen the evidence, we showed that opsonization of PS-COOH and PS-NH_2 with IgG is likewise sufficient to shift the uptake mechanism in protein-free medium from clathrin-mediated endocytosis (PS-COOH) and macropinocytosis (PS-NH_2) (Figure 3D, Supporting Information, Figure S3A,B) to phagocytosis of both particles (Figure 6E). Hence, absorption of antibodies alone changes the uptake behavior of macrophages from macropinocytic and endocytic in buffer to phagocytic mechanism.

Opsonization also had an impact on nanoparticle uptake by THP-1 cells and PMA-differentiated THP-1 cells, changing their uptake mechanism from macropinocytosis and clathrin- and dynamin-dependent endocytosis to clathrin-independent dynamin-dependent endocytosis for THP-1 cells and PS-COOH; clathrin-dependent scavenger receptor A-mediated endocytosis to macropinocytosis for differentiated THP-1 cells. Similarly, others have shown uptake of commercially available negatively charged polystyrene nanoparticles by scavenger receptor MARCO-transfected COS cells.[54]

Particle Distribution in an *in Vivo* Model. We further analyzed the distribution of PS-COOH and PS-NH_2 nanoparticles in an *in vivo* model. A tumor cell xenograft was transplanted on the chick chorioallantoic membrane (CAM) of fertilized chicken eggs. Two days later, the particles were injected intravenously. After four days, the particle distribution was analyzed in tumor xenografts and in embryonic liver tissue, which contains liver macrophages, so-called Kupffer cells, which represent 15% of the liver cell population and 50% of all resident macrophages in the body.[55] In agreement with the *in vitro* studies, intravenously injected PS-COOH was found predominantly in the chicken liver, where macrophages of the reticuloendothelial system reside. By contrast, the PS-NH_2 particles were found to accumulate in the tumor xenografts (Figure 7A,B). Staining for the macrophage marker KUL01 revealed that, in liver tissue, both particles were confined to macrophages (Figure 7C). In tumor tissue, PS-COOH particles were accumulated by macrophages, whereas PS-NH_2 were taken up by both, macrophages and tumor cells (Figure 7D).

Thus, compared to macrophages, the undifferentiated monocytic THP-1 cells as well as PMA-differentiated THP-1 cells utilize different mechanisms to internalize nanoparticles. Therefore, we conclude that, while a cell line might be highly valuable to address questions concerning tumor cell targeting, its use as a model for primary cells is not necessarily warranted, but requires profound validation with primary cells.

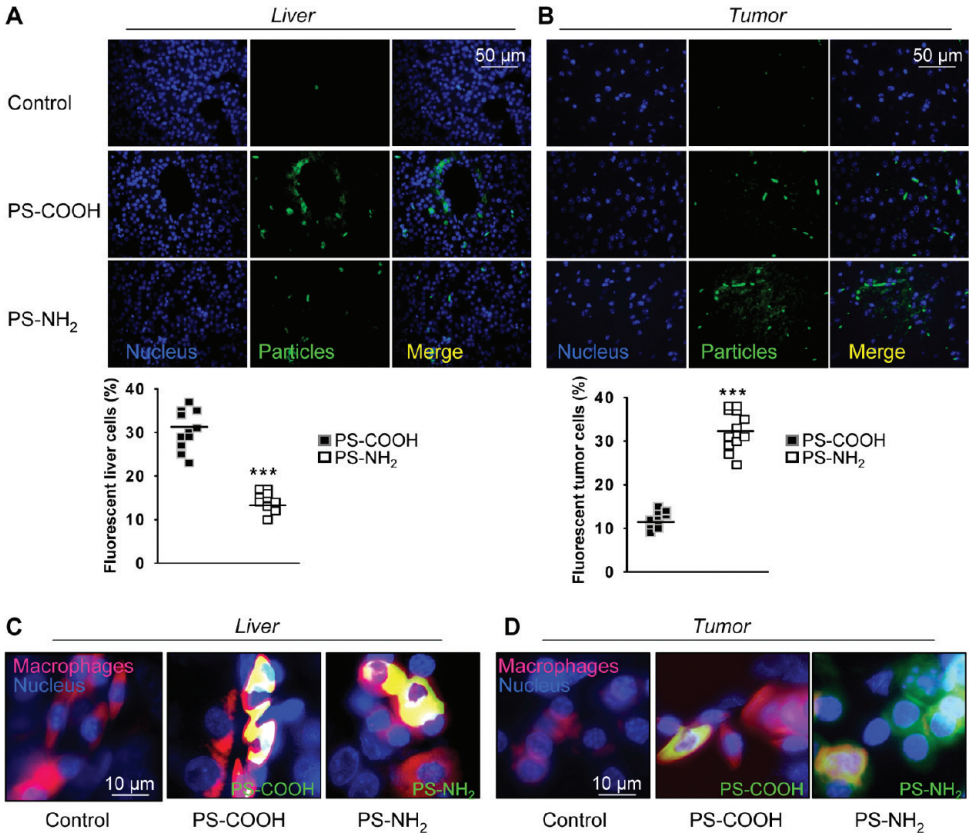

Figure 7. Differential accumulation of the carboxy and amino functionalized polystyrene nanoparticles in liver and tumor tissues. Adherently growing PC-3 prostate cancer cells (0.5×10^6 cells) were grafted onto the chorioallantoic membrane of chicken eggs 6 days after fertilization. After 2 days, the eggs were intravenously injected with 50 μg/kg of either particle in 100 μL of 0.9% NaCl. After 4 days, livers and tumor xenografts were collected, paraffin-embedded, and sectioned. Nuclei were counterstained with DAPI, and the sections were analyzed by fluorescent microscopy (original magnification, 200×). Representative fluorescence images of liver (A) and tumors (B) are shown. Fluorescently labeled cells of three sections were quantified for each egg. Results are presented as mean ± SEM of four eggs in each group: (***) $p < 0.001$. The data shown are representative of four eggs each. Fluorescently labeled nanoparticles colocalize with macrophages in liver (C) and tumor tissues (D). Tissue sections were processed and stained for chicken macrophage marker KUL01 (red), nuclei were counterstained with DAPI (blue), nanoparticles (green), colocalization (yellow). Representative images are shown (original magnification, 1000×).

CONCLUSION

Our study shows that the (i) extent of nanoparticle internalization, (ii) kinetics of particle uptake, and (iii) particle uptake mechanisms may grossly differ between primary cells, phenotypically related tumor cell lines, and thereof derived differentiated tumor cells. All these processes depend critically on the surface charge of the nanoparticles and their opsonization by serum proteins. Our findings indicate that results obtained from studies of nanoparticle−cell interactions on cell line models may not be applicable to the situation in normal differentiated cells.

MATERIALS AND METHODS

Preparation of Polystyrene Nanoparticles. Two types of fluorescent cationic nanoparticles were synthesized by the miniemulsion polymerization process.[28,29] For the synthesis of PS nanoparticles, 6 g of freshly distilled styrene (Merck), 250 mg of hexadecane (Sigma-Aldrich, Taufkirchen, Germany), 5 mg of the fluorescent dye *N*-(2,6-diisopropylphenyl)-perylene-3,4-dicarbonacidimide (PMI, BASF, Ludwigshafen, Germany), and 100 mg of the hydrophobic initiator 2,2′-azobis(2-methylbutyronitrile) (V59, Wako Chemicals, Neuss, Germany) were added to 24 g of water containing 125 mg of the surfactant cetyltrimethylammonium chloride. After stirring 1 h for pre-emulsification, the miniemulsion was prepared by sonification for 120 s at 90% amplitude (Branson sonifier W450 Digital, $^1/_2$ in. tip) at 0 °C to prevent polymerization. Polymerization was carried out at 72 °C overnight. After the synthesis, surfactant was removed by Amicon ultrafiltration (100 kDa), extensive dialysis and washing. Before being used, the particle suspensions were dispersed by sonification and the absence of agglomeration was controlled by a Zetasizer Nano (Malvern Instruments, UK).

Physicochemical Characterization of the Nanoparticles. The average particle size, polydispersity index (PDI), and zeta potential were determined by dynamic light scattering (DLS) in 1 mM KCl solution at pH 7.0 using a Zetasizer Nano. The intensity of the scattered light was measured at 173° to the incident beam. Incorporated PMI was quantified by UV−vis absorption spectroscopy (Lambda 16, Perkin-Elmer, Rodgau, Germany) of the dried nanoparticles dissolved in tetrahydrofuran. Both, carboxy

(PS-COOH) and amino (PS-NH_2) functionalized polystyrene particles contained the same amount of dye, which enabled quantification of the uptake experiments with particle comparison. The surface charge density was determined by polyelectrolyte titration using a particle charge detector PCD 02 (Muetek, Germany) in combination with a 702 SM Titrino automatic titrator (Metrohm, Switzerland).[29]

Cell Differentiation and Measurement of Viability. Macrophages were differentiated from human monocytes isolated from buffy coats by density gradient centrifugation and differentiated as described earlier.[56,57] Human monocytic leukemia cell line THP-1 (American Type Culture Collection) was grown in RPMI 1640 medium supplemented with 10% FCS in a humidified 5% CO_2 atmosphere at 37 °C. Cells (2×10^5 cells/mL) were differentiated using 200 nM PMA (Sigma-Aldrich) for 3 days followed by 5 days in medium without PMA.[16] Cell viability was analyzed by mitochondrial reduction of XTT (Roche Diagnostics, Basel, Switzerland). For the analysis of lysosomal leakage, the cells were stained with acridine orange (AO) and analyzed by flow cytometry to detect the population of AO^{low} cells.[14]

Nanoparticle Uptake Studies. Uptake was analyzed either in HBSS or in RPMI 1640 medium supplemented with 10% human AB serum. Macrophages and THP-1 cells (1×10^6 cells/mL) were preincubated with different pharmacological pathway inhibitors (scavenger receptor, 10 μg/mL polyinosinic acid for 30 min;[32] macropinocytosis, 2 μM rottlerin for 30 min;[39] pinocytosis, 100 μg/mL colchicine for 2 h;[40] phagocytosis, 10 μg/mL cytochalasin B for 2 h;[40] clathrin-mediated endocytosis, 200 μM monodansyl cadaverine for 10 min;[41] caveolae-mediated endocytosis, 50 μg/mL nystatin for 15 min;[42] dynamin-dependent endocytosis, 80 μM dynasore for 30 min,[43] and treated with 100 μg/mL of either particle for 6 h. We have also used 10 μM nocodazole for 30 min as an inhibitor of pinocytosis,[45] 100 μM dimethylamiloride for 30 min as an inhibitor of macropinocytosis,[46] and 0.5 μM latrunculin A for 30 min to inhibit phagocytosis.[47] The inhibitors were not removed during the uptake experiments.

Nanoparticle uptake was analyzed by flow cytometry (Becton Dickinson, Franklin Lakes, NJ); at least 10 000 cells were counted. The data were presented as mean fluorescence index (MFI) and calculated as the ratio of the mean fluorescence intensity of the sample and the control. The specificity of the pharmacological inhibition of the uptake processes was validated using fluorescent human transferrin and *Escherichia coli* K-12 BioParticles (Invitrogen).

Western Immunoblot Analysis of Protein Expression. Aliquots of whole cell lysates were separated by SDS-PAGE, transferred, and probed with specific antibodies against CD64 (Dako, Glostrup, Denmark), dynamin I/II (Cell Signaling), scavenger receptor A (R&D Systems) and clathrin (Santa Cruz) as described;[58,59] actin (Chemicon) staining served as loading control. The surface expression of CD64 and scavenger receptor A was analyzed by flow cytometry using corresponding antibodies and PE-conjugated secondary $F(ab')_2$ from Dianova (Hamburg, Germany).

Nanoparticle−Protein Interaction. Nanoparticles (100 μg/mL) were incubated either in HBSS, in RPMI 1640 medium supplemented with 10% human AB serum for 1 h or 10 mg/mL human IgG for 2 h at 37 °C. The particles were collected by centrifugation and washed extensively with PBS. IgG-precoated particles were added to macrophages pretreated with different phagocytosis inhibitors, and the cells were analyzed by flow cytometry. The proteins associated with the particles were eluted and denaturated in sample loading buffer and separated by gel electrophoresis. As control, 5 μL of human AB serum, 0.5 μg of human IgG, and 25 μg of albumin (HA) were used. Gels were stained with Coomassie blue or blotted onto a PVDF membrane and stained with antihuman IgG-HRP (Jackson Laboratories).

Confocal Microscopy. Macrophages and THP-1 cells were incubated with the functionalized polystyrene nanoparticles (100 μg/mL) in either HBSS or in RPMI 1640 medium supplemented with 10% human AB serum for 2 h and analyzed by confocal microscopy. Cell membranes were labeled with CellMask (Invitrogen). Fluorescence images were taken with the acquisition software Andor iQ 1.6.[43,57]

Knockdown of CD64, Dynamin, and Clathrin. For *in vitro* knockdown of CD64, dynamin I, dynamin II, and clathrin, phosphorothioate-modified oligodeoxynucleotides (ODN) (ThermoHybaid, Ulm, Germany) were used. The ODN sequences complementary to corresponding mRNA sequences devoid of secondary structures, such as the loops, were selected using available algorithms.[60] The antisense ODN for high affinity FcγRI (CD64) corresponded to the nucleotides 1383−1404 of human CD64 mRNA (NM_000566.3) 5′-TAAAGAATTCTTGAAAAACTTA-3′, for human dynamin I they corresponded to the nucleotides 309−332 (NM_001005336) 5′-AACCACAGAATATGCCGA-3′, and for human dynamin II they corresponded to nucleotides 1338−1355 (NM_001005362.1) 5′-ATTAAGAACATCCATGGA-3′. The antisense ODN for clathrin corresponded to nucleotides 1672−1691 of human clathrin mRNA (NM_004859) 5′- AAACTTCTCCTCTACTTCA-3′. The control sequences contained the same set of the base pairs in a scrambled order. The sequences were analyzed for lack of secondary structure and oligo pairing. According to Blast search, the selected sequences did not show any similarity to any coding mRNA sequence. Macrophages were treated for 48 h every 24 h with 10 μM of the ODN in RPMI 1620 supplemented with 10% FCS.[61] THP-1 cells were preconditioned for 4 h in medium without FCS and treated with 10 μM of the ODN in the same medium. The medium was supplemented with 10% FCS 4 h later, and the cells were incubated for an additional 20 h. The cells were either lysed and analyzed for protein expression by Western immunoblotting using antibodies against CD64 (Dako), dynamin I/II (Cell Signaling), or clathrin (Santa Cruz) or incubated with the nanoparticles (each 100 μg/mL) for 6 h. Particle uptake was analyzed using flow cytometry as described above.

***In Vivo* Biodistribution of Polystyrene Nanoparticles.** PC-3 cells (American Type Culture Collection) were cultured in Ham's F-12-K medium supplemented with 10% FCS. For xenotransplantation, 0.5×10^6 cells in the log growth phase were seeded in 20 μL of medium/Matrigel (1:1, v/v) into a 6-mm silicone ring placed onto the chick chorioallantoic membrane (CAM) of fertilized chicken eggs and incubated at 37 °C and constant humidity.[62] After 2 days, the eggs were intravenously injected with 50 μg/kg of either particle in 100 μL 0.9% NaCl. After 4 days, liver and tumor tissues were collected, embedded in paraffin and sectioned. Sections were processed and stained for the chicken macrophage marker KUL01 (Novus Biologicals), nuclei were counterstained with DAPI, and the sections were analyzed by fluorescence microscopy. The images were digitally recorded with an Axiophot microscope (Carl Zeiss, Jena, Germany) and a Sony MC-3249 CCD camera using Visupac 22.1 software (Carl Zeiss).

Statistical Analysis. Quantitative results are expressed as mean ± SEM. Results were analyzed by multigroup comparison Mann−Whitney U and Newman-Keuls tests. Differences were considered statistically significant at $p < 0.05$.

Acknowledgment. This work was supported by the Deutsche Forschungsgemeinschaft (DFG) through the Priority Program SPP1313 and the Center for Functional Nanostructures (CFN).

Supporting Information Available: Confocal photomicrographs of the used cell types, effects of pharmacological inhibitors on cell viability and particle uptake. This material is available free of charge *via* the Internet at http://pubs.acs.org.

REFERENCES AND NOTES

1. Xie, J.; Huang, J.; Li, X.; Sun, S.; Chen, X. Iron Oxide Nanoparticle Platform for Biomedical Applications. *Curr. Med. Chem.* **2009,** *16*, 1278–1294.
2. Moghimi, S. M.; Hunter, A. C.; Murray, J. C. Nanomedicine: Current Status and Future Prospects. *FASEB J.* **2005,** *19*, 311–330.
3. Mora-Huertas, C. E.; Fessi, H.; Elaissari, A. Polymer-Based Nanocapsules for Drug Delivery. *Int. J. Pharm.* **2010,** *385*, 113–142.
4. Boczkowski, J.; Hoet, P. What's New in Nanotoxicology? Implications for Public Health from a Brief Review of the 2008 Literature. *Nanotoxicology* **2010,** *4*, 1–14.

5. Kim, B. Y.; Rutka, J. T.; Chan, W. C. Nanomedicine. *New. Engl. J. Med.* **2010,** *363*, 2434–2443.
6. Mosser, D. M.; Edwards, J. P. Exploring the Full Spectrum of Macrophage Activation. *Nat. Rev. Immunol.* **2008,** *8*, 958–969.
7. Hillaireau, H.; Couvreur, P. Nanocarriers' Entry into the Cell: Relevance to Drug Delivery. *Cell. Mol. Life Sci.* **2009,** *66*, 2873–2896.
8. Chellat, F.; Merhi, Y.; Moreau, A.; Yahia, L. Therapeutic Potential of Nanoparticulate Systems for Macrophage Targeting. *Biomaterials* **2005,** *26*, 7260–7275.
9. Amor, S.; Puentes, F.; Baker, D.; van der Valk, P. Inflammation in Neurodegenerative Diseases. *Immunology* **2010,** *129*, 154–169.
10. Swanson, J. A. Shaping Cups into Phagosomes and Macropinosomes. *Nat. Rev. Mol. Cell. Biol.* **2008,** *9*, 639–649.
11. Lunov, O.; Syrovets, T.; Röcker, C.; Tron, K.; Nienhaus, G. U.; Rasche, V.; Mailänder, V.; Landfester, K.; Simmet, T. Lysosomal Degradation of the Carboxydextran Shell of Coated Superparamagnetic Iron Oxide Nanoparticles and the Fate of Professional Phagocytes. *Biomaterials* **2010,** *31*, 9015–9022.
12. Abrink, M.; Gobl, A. E.; Huang, R.; Nilsson, K.; Hellman, L. Human Cell Lines U-937, THP-1 and Mono Mac 6 Represent Relatively Immature Cells of the Monocyte−Macrophage Cell Lineage. *Leukemia* **1994,** *8*, 1579–1584.
13. Xia, T.; Kovochich, M.; Brant, J.; Hotze, M.; Sempf, J.; Oberley, T.; Sioutas, C.; Yeh, J. I.; Wiesner, M. R.; Nel, A. E. Comparison of the Abilities of Ambient and Manufactured Nanoparticles to Induce Cellular Toxicity According to an Oxidative Stress Paradigm. *Nano. Lett.* **2006,** *6*, 1794–1807.
14. Xia, T.; Kovochich, M.; Liong, M.; Zink, J. I.; Nel, A. E. Cationic Polystyrene Nanosphere Toxicity Depends on Cell-Specific Endocytic and Mitochondrial Injury Pathways. *ACS Nano* **2008,** *2*, 85–96.
15. Schwende, H.; Fitzke, E.; Ambs, P.; Dieter, P. Differences in the State of Differentiation of THP-1 Cells Induced by Phorbol Ester and 1,25-Dihydroxyvitamin D3. *J. Leukoc. Biol.* **1996,** *59*, 555–561.
16. Daigneault, M.; Preston, J. A.; Marriott, H. M.; Whyte, M. K.; Dockrell, D. H. The Identification of Markers of Macrophage Differentiation in PMA-Stimulated THP-1 Cells and Monocyte-Derived Macrophages. *PLoS One* **2010,** *5*, e8668.
17. Kohro, T.; Tanaka, T.; Murakami, T.; Wada, Y.; Aburatani, H.; Hamakubo, T.; Kodama, T. A Comparison of Differences in the Gene Expression Profiles of Phorbol 12-Myristate 13-Acetate Differentiated THP-1 Cells and Human Monocyte-Derived Macrophage. *J. Atheroscler. Thromb.* **2004,** *11*, 88–97.
18. Velev, O. D.; Kaler, E. W. *In Situ* Assembly of Colloidal Particles into Miniaturized Biosensors. *Langmuir* **1999,** *15*, 3693–3698.
19. Rogach, A.; Susha, A.; Caruso, F.; Sukhorukov, G.; Kornowski, A.; Kershaw, S.; Möhwald, H.; Eychmüller, A.; Weller, H. Nano- and Microengineering: 3-D Colloidal Photonic Crystals Prepared from Sub-mm-Sized Polystyrene Latex Spheres Precoated with Luminescent Polyelectrolyte/Nanocrystal Shells. *Adv. Mater.* **2000,** *12*, 333–337.
20. Boal, A. K.; Ilhan, F.; DeRouchey, J. E.; Thurn-Albrecht, T.; Russell, T. P.; Rotello, V. M. Self-Assembly of Nanoparticles into Structured Spherical and Network Aggregates. *Nature* **2000,** *404*, 746–748.
21. Florence, A. T. Issues in Oral Nanoparticle Drug Carrier Uptake and Targeting. *J. Drug Target.* **2004,** *12*, 65–70.
22. Yu, S.; Chow, G. M. Carboxyl Group (−CO_2H) Functionalized Ferrimagnetic Iron Oxide Nanoparticles for Potential Bio-Applications. *J. Mater. Chem.* **2004,** *14*, 2781–2786.
23. Nel, A. E.; Madler, L.; Velegol, D.; Xia, T.; Hoek, E. M.; Somasundaran, P.; Klaessig, F.; Castranova, V.; Thompson, M. Understanding Biophysicochemical Interactions at the Nano−Bio Interface. *Nat. Mater.* **2009,** *8*, 543–557.
24. Qian, J.; Wang, Y.; Gao, X.; Zhan, Q.; Xu, Z.; He, S. Carboxyl-Functionalized and Bio-Conjugated Silica-Coated Quantum Dots as Targeting Probes for Cell Imaging. *J. Nanosci. Nanotechnol.* **2010,** *10*, 1668–1675.
25. Godbey, W. T.; Wu, K. K.; Mikos, A. G. Poly(Ethylenimine) and Its Role in Gene Delivery. *J. Controlled Release* **1999,** *60*, 149–160.
26. Lim, Y.; Kim, S. M.; Lee, Y.; Lee, W.; Yang, T.; Lee, M.; Suh, H.; Park, J. Cationic Hyperbranched Poly(Amino Ester): A Novel Class of DNA Condensing Molecule with Cationic Surface, Biodegradable Three-Dimensional Structure, and Tertiary Amine Groups in the Interior. *J. Am. Chem. Soc.* **2001,** *123*, 2460–2461.
27. Fang, C.; Bhattarai, N.; Sun, C.; Zhang, M. Functionalized Nanoparticles with Long-Term Stability in Biological Media *Small* **2009,** *5*, 1637–1641.
28. Holzapfel, V.; Musyanovych, A.; Landfester, K.; Lorenz, M. R.; Mailänder, V. Preparation of Fluorescent Carboxyl and Amino Functionalized Polystyrene Particles by Miniemulsion Polymerization as Markers for Cells. *Macromol. Chem. Phys.* **2005,** *206*, 2440–2449.
29. Musyanovych, A.; Rossmanith, R.; Tontsch, C.; Landfester, K. Effect of Hydrophilic Comonomer and Surfactant Type on the Colloidal Stability and Size Distribution of Carboxyl- and Amino-Functionalized Polystyrene Particles Prepared by Miniemulsion Polymerization. *Langmuir* **2007,** *23*, 5367–5376.
30. Briley-Saebo, K. C.; Johansson, L. O.; Hustvedt, S. O.; Haldorsen, A. G.; Bjornerud, A.; Fayad, Z. A.; Ahlstrom, H. K. Clearance of Iron Oxide Particles in Rat Liver: Effect of Hydrated Particle Size and Coating Material on Liver Metabolism. *Invest. Radiol.* **2006,** *41*, 560–571.
31. Garcia-Garcia, E.; Rosales, R.; Rosales, C. Phosphatidylinositol 3-Kinase and Extracellular Signal-Regulated Kinase Are Recruited for Fc Receptor-Mediated Phagocytosis During Monocyte-to-Macrophage Differentiation. *J. Leukoc. Biol.* **2002,** *72*, 107–114.
32. Raynal, I.; Prigent, P.; Peyramaure, S.; Najid, A.; Rebuzzi, C.; Corot, C. Macrophage Endocytosis of Superparamagnetic Iron Oxide Nanoparticles: Mechanisms and Comparison of Ferumoxides and Ferumoxtran-10. *Invest. Radiol.* **2004,** *39*, 56–63.
33. Morishige, T.; Yoshioka, Y.; Tanabe, A.; Yao, X.; Tsunoda, S.; Tsutsumi, Y.; Mukai, Y.; Okada, N.; Nakagawa, S. Titanium Dioxide Induces Different Levels of IL-1β Production Dependent on Its Particle Characteristics through Caspase-1 Activation Mediated by Reactive Oxygen Species and Cathepsin B. *Biochem. Biophys. Res. Commun.* **2010,** *392*, 160–165.
34. Janic, B.; Iskander, A. S.; Rad, A. M.; Soltanian-Zadeh, H.; Arbab, A. S. Effects of Ferumoxides-Protamine Sulfate Labeling on Immunomodulatory Characteristics of Macrophage-Like THP-1 Cells. *PLoS One* **2008,** *3*, e2499.
35. Röcker, C.; Potzl, M.; Zhang, F.; Parak, W. J.; Nienhaus, G. U. A Quantitative Fluorescence Study of Protein Monolayer Formation on Colloidal Nanoparticles. *Nat. Nanotechnol.* **2009,** *4*, 577–580.
36. Jiang, X.; Weise, S.; Hafner, M.; Röcker, C.; Zhang, F.; Parak, W. J.; Nienhaus, G. U. Quantitative Analysis of the Protein Corona on FePt Nanoparticles Formed by Transferrin Binding. *J. R. Soc. Interface* **2010,** *7* (Suppl 1), S5–S13.
37. Bultel, S.; Helin, L.; Clavey, V.; Chinetti-Gbaguidi, G.; Rigamonti, E.; Colin, M.; Fruchart, J. C.; Staels, B.; Lestavel, S. Liver X Receptor Activation Induces the Uptake of Cholesteryl Esters from High Density Lipoproteins in Primary Human Macrophages. *Arterioscler. Thromb. Vasc. Biol.* **2008,** *28*, 2288–2295.
38. Veiga, E.; Cossart, P. The Role of Clathrin-Dependent Endocytosis in Bacterial Internalization. *Trends Cell Biol.* **2006,** *16*, 499–504.
39. Sarkar, K.; Kruhlak, M. J.; Erlandsen, S. L.; Shaw, S. Selective Inhibition by Rottlerin of Macropinocytosis in Monocyte-Derived Dendritic Cells. *Immunology* **2005,** *116*, 513–524.
40. Dunning, M. D.; Lakatos, A.; Loizou, L.; Kettunen, M.; ffrench-Constant, C.; Brindle, K. M.; Franklin, R. J. Superparamagnetic Iron Oxide-Labeled Schwann Cells and Olfactory Ensheathing Cells Can Be Traced *in Vivo* by Magnetic Resonance Imaging and Retain Functional Properties after Transplantation into the CNS. *J. Neurosci.* **2004,** *24*, 9799–9810.

41. Panicker, A. K.; Buhusi, M.; Erickson, A.; Maness, P. F. Endocytosis of β1 Integrins Is an Early Event in Migration Promoted by the Cell Adhesion Molecule L1. *Exp. Cell Res.* **2006,** *312*, 299–307.
42. Ros-Baro, A.; Lopez-Iglesias, C.; Peiro, S.; Bellido, D.; Palacin, M.; Zorzano, A.; Camps, M. Lipid Rafts Are Required for Glut4 Internalization in Adipose Cells. *Proc. Natl. Acad. Sci. U.S.A.* **2001,** *98*, 12050–12055.
43. Jiang, X.; Dausend, J.; Hafner, M.; Musyanovych, A.; Röcker, C.; Landfester, K.; Mailander, V.; Nienhaus, G. U. Specific Effects of Surface Amines on Polystyrene Nanoparticles in Their Interactions with Mesenchymal Stem Cells. *Biomacromolecules* **2010,** *11*, 748–753.
44. Yacobi, N. R.; Malmstadt, N.; Fazlollahi, F.; DeMaio, L.; Marchelletta, R.; Hamm-Alvarez, S. F.; Borok, Z.; Kim, K. J.; Crandall, E. D. Mechanisms of Alveolar Epithelial Translocation of a Defined Population of Nanoparticles. *Am. J. Respir. Cell Mol. Biol.* **2010,** *42*, 604–614.
45. Sen, D.; Deerinck, T. J.; Ellisman, M. H.; Parker, I.; Cahalan, M. D. Quantum Dots for Tracking Dendritic Cells and Priming an Immune Response *in Vitro* and *in Vivo*. *PLoS One* **2008,** *3*, e3290.
46. Goncalves, C.; Mennesson, E.; Fuchs, R.; Gorvel, J. P.; Midoux, P.; Pichon, C. Macropinocytosis of Polyplexes and Recycling of Plasmid *via* the Clathrin-Dependent Pathway Impair the Transfection Efficiency of Human Hepatocarcinoma Cells. *Mol. Ther.* **2004,** *10*, 373–385.
47. Oliveira, C. A.; Kashman, Y.; Mantovani, B. Effects of Latrunculin a on Immunological Phagocytosis and Macrophage Spreading-Associated Changes in the F-Actin/G-Actin Content of the Cells. *Chem. Biol. Interact.* **1996,** *100*, 141–153.
48. Lakadamyali, M.; Rust, M. J.; Zhuang, X. Ligands for Clathrin-Mediated Endocytosis Are Differentially Sorted into Distinct Populations of Early Endosomes. *Cell* **2006,** *124*, 997–1009.
49. Dobrovolskaia, M. A.; McNeil, S. E. Immunological Properties of Engineered Nanomaterials. *Nat. Nanotechnol.* **2007,** *2*, 469–478.
50. Sontag, J. M.; Fykse, E. M.; Ushkaryov, Y.; Liu, J. P.; Robinson, P. J.; Sudhof, T. C. Differential Expression and Regulation of Multiple Dynamins. *J. Biol. Chem.* **1994,** *269*, 4547–4554.
51. Jones, S. M.; Howell, K. E.; Henley, J. R.; Cao, H.; McNiven, M. A. Role of Dynamin in the Formation of Transport Vesicles from the Trans-Golgi Network. *Science* **1998,** *279*, 573–577.
52. Nimmerjahn, F.; Ravetch, J. V. Fc-Receptors as Regulators of Immunity. *Adv. Immunol.* **2007,** *96*, 179–204.
53. Gessner, A.; Lieske, A.; Paulke, B. R.; Muller, R. H. Functional Groups on Polystyrene Model Nanoparticles: Influence on Protein Adsorption. *J. Biomed. Mater. Res. A* **2003,** *65*, 319–326.
54. Kanno, S.; Furuyama, A.; Hirano, S. A Murine Scavenger Receptor Marco Recognizes Polystyrene Nanoparticles. *Toxicol. Sci.* **2007,** *97*, 398–406.
55. Si-Tayeb, K.; Lemaigre, F. P.; Duncan, S. A. Organogenesis and Development of the Liver. *Dev. Cell* **2010,** *18*, 175–189.
56. Colognato, R.; Slupsky, J. R.; Jendrach, M.; Burysek, L.; Syrovets, T.; Simmet, T. Differential Expression and Regulation of Protease-Activated Receptors in Human Peripheral Monocytes and Monocyte-Derived Antigen-Presenting Cells. *Blood* **2003,** *102*, 2645–2652.
57. Lunov, O.; Syrovets, T.; Büchele, B.; Jiang, X.; Röcker, C.; Tron, K.; Nienhaus, G. U.; Walther, P.; Mailänder, V.; Landfester, K.; *et al*. The Effect of Carboxydextran-Coated Superparamagnetic Iron Oxide Nanoparticles on C-Jun N-Terminal Kinase-Mediated Apoptosis in Human Macrophages. *Biomaterials* **2010,** *31*, 5063–5071.
58. Syrovets, T.; Jendrach, M.; Rohwedder, A.; Schüle, A.; Simmet, T. Plasmin-Induced Expression of Cytokines and Tissue Factor in Human Monocytes Involves AP-1 and IKKβ-Mediated NF-κB Activation. *Blood* **2001,** *97*, 3941–3950.
59. Burysek, L.; Syrovets, T.; Simmet, T. The Serine Protease Plasmin Triggers Expression of MCP-1 and CD40 in Human Primary Monocytes *via* Activation of P38 MAPK and Janus Kinase (Jak)/Stat Signaling Pathways. *J. Biol. Chem.* **2002,** *277*, 33509–33517.
60. Zuker, M. Mfold Web Server for Nucleic Acid Folding and Hybridization Prediction. *Nucleic Acids Res.* **2003,** *31*, 3406–3415.
61. Laumonnier, Y.; Syrovets, T.; Burysek, L.; Simmet, T. Identification of the Annexin A2 Heterotetramer as a Receptor for the Plasmin-Induced Signaling in Human Peripheral Monocytes. *Blood* **2006,** *107*, 3342–3349.
62. Syrovets, T.; Gschwend, J. E.; Büchele, B.; Laumonnier, Y.; Zugmaier, W.; Genze, F.; Simmet, T. Inhibition of IκB Kinase Activity by Acetyl-Boswellic Acids Promotes Apoptosis in Androgen-Independent PC-3 Prostate Cancer Cells *in Vitro* and *in Vivo*. *J. Biol. Chem.* **2005,** *280*, 6170–6180.